Incorporation of Si^{4+}–N^{3-} into Ce^{3+} -Doped Garnets for Warm White LED Phosphors

Anant A. Setlur,*,† William J. Heward,† Mark E. Hannah,‡ and Uwe Happek‡

GE Global Research, 1 Research Circle, Niskayuna, New York 12309, and Department of Physics and Astronomy, University of Georgia, Athens, Georgia 30602

Received June 25, 2008

The effect of $Si^{4+}-N^{3-}$ incorporation on Ce^{3+} doped $RE_3Al_5O_{12}:Ce^{3+}$ (RE = Lu^{3+}, Y^{3+}, or Tb^{3+}) garnet phosphors is described in this report. The addition of $Si^{4+}-N^{3-}$ leads to distinct low-energy Ce^{3+} absorption and emission bands that are assigned to Ce^{3+} ions that have N^{3-} in their local coordination. The combination of the typical Ce^{3+} emission in garnets with the low energy Ce^{3+} emission band results in a broad emission spectrum suited for white LED lamps with low color temperatures and good color rendering using only a single phosphor. The low-energy Ce^{3+} emission band has stronger quenching at high temperatures, a potential limitation. The mechanism for this quenching is discussed.

1. Introduction

Efficacies for commercial phosphor converted LEDs (pcLEDs) using blue InGaN LEDs and $Y_3Al_5O_{12}:Ce^{3+}$ (YAG:Ce) garnet-based phosphors can be greater than 80 lm/W for 1 W devices.[1−3] These efficacies are higher than compact fluorescent lamps (CFLs) and comparable to linear fluorescent lamps, and implementation of high efficacy pcLED lamps into general lighting could significantly reduce lighting energy consumption. However, other requirements, such as lamp color, need to be met before pcLEDs can extensively replace fluorescent or incandescent light sources. For example, the highest efficacy pcLED lamps have color temperatures (CCTs) of 4500−6500 K, making them less acceptable as replacements for incandescent and halogen lamps that have CCTs of 2500−3200 K. In addition, for CCTs less than 6000 K, the color rendering index (CRI) of typical high efficacy pcLED lamps is less than 80, in comparison to CRIs of 100 for incandescent and halogen lamps (by definition) and ∼82−85 for CFLs. Achieving lower CCTs and higher CRIs requires red phosphors to compensate for the spectral deficiencies of standard pcLEDs. There has been significant effort toward red phosphor development resulting in efficient Eu^{2+} and Ce^{3+} phosphors, such as $(Sr,Ca)S:Eu^{2+}$,[4] $(Ba,Sr,Ca)_2Si_5N_8:Eu^{2+}$,[5] $CaAlSiN_3:Eu^{2+}$,[6] and $Lu_2CaMg_2Si_3O_{12}:Ce^{3+}$,[7] that can meet some of the red spectral requirements for general illumination lighting. However, these phosphors have to be blended with YAG:Ce-based phosphors to make white lamps, possibly leading to variations during lamp manufacturing.

In principle, using a single white phosphor instead of phosphor blends could help to reduce some of this variability. One approach leading to a single good CRI/low CCT phosphor is a modification of the composition of Ce^{3+}-doped garnets by creating additional "sites" for Ce^{3+} with redder emission while retaining part of the typical yellow-green Ce^{3+} emission in aluminate garnets. The Ce^{3+} emission can be strongly red-shifted when there is a larger crystal field splitting of the two lowest-energy $5d^1$ levels, as in $Lu_2CaMg_2Si_3O_{12}$.[7] There is a distribution of higher and lower energy Ce^{3+} sites in this silicate garnet, but this does not lead to a single low CCT/good CRI phosphor due to inhomogeneous broadening that smears any distinction between high and low energy sites. Because the energy position of the lowest Ce^{3+} $5d^1$ level can be modified by the covalency and polarizability of Ce^{3+}−ligand bonds,[8] incorporating ligands with a lower electronegativity compared to O^{2-} ($\chi(O) \approx 3.4$) would lower the energy of the $5d^1$ levels and lead to distinct Ce^{3+} sites with redder emission. One example where incorporating ligands with lower electronegativity leads to a redshift in $4f^{N-1}5d^1 \rightarrow 4f^N$ emission is $(Sr,Ba,Ca)Al_{2-x}Si_xO_{4-x}N_x:Eu^{2+}$,[9] where O^{2-} anions are replaced by N^{3-} ($\chi(N) \approx 3.0$) with Si^{4+} charge compensation. A similar incorporation of N^{3-} in YAG has been reported in ceramic sintering experiments with Si_2N_2O as the $Si^{4+}-N^{3-}$ source.[10] In this report, it is shown that the incorporation of $Si^{4+}-N^{3-}$ into aluminate garnets leads to phosphors with two main sites for Ce^{3+} luminescence:

* Corresponding author. E-mail: setlur@research.ge.com.
† GE Global Research.
‡ University of Georgia.

(1) Krames, M. R.; Shchekin, O. B.; Mueller-Mach, R.; Mueller, G. O.; Zhou, L.; Harbers, G.; Craford, M. G. *J. Display Technol.* **2007**, *3*, 160.
(2) Schubert, E. F.; Kim, J. K. *Science* **2005**, *308*, 1274.
(3) Narukawa, Y.; Narita, J.; Sakamoto, T.; Deguchi, K.; Yamada, T.; Mukai, T. *Jpn. J. Appl. Phys.* **2006**, *45*, L1084.
(4) Mueller-Mach, R.; Mueller; G, O.; Krames, M. R.; Trottier, T. *IEEE J. Sel. Top. Quantum Electron.* **2002**, *8*, 339.
(5) Li, Y. Q.; van Steen, J. E. J.; van Krevel, J. W. H.; Botty, G.; Delsing, A. C. A.; DiSalvo, F. J.; de With, G.; Hintzen, H. T. *J. Alloys Compd.* **2006**, *417*, 273.
(6) Uheda, K.; Hirosaki, N.; Yamamoto, Y.; Naito, A.; Nakajima, T.; Yamamoto, H. *Electrochem.Solid-State Lett.* **2006**, *9*, H22.
(7) Setlur, A. A.; Heward, W. J.; Gao, Y.; Srivastava, A. M.; Chandran, R. G.; Shankar, M. V. *Chem. Mater.* **2006**, *18*, 3314.
(8) Dorenbos, P. *Phys. Rev. B* **2001**, *64*, 125117.
(9) Li, Y. Q.; de With, G.; Hintzen, H. T. *J. Electrochem. Soc.* **2006**, *153*, G278.
(10) Sun, W. Y.; Li, X. T.; Ma, L. T.; Yen, T. S. *J. Solid State Chem.* **1984**, *51*, 315.

10.1021/cm801732d CCC: $40.75
Published on Web 09/19/2008

"typical" Ce^{3+} ions in the Al^{3+} garnets and a site with a red-shifted Ce^{3+} $4f^1 \rightarrow 5d^1$ absorption and $5d^1 \rightarrow 4f^1$ emission bands that are attributed to Ce^{3+} ions with N^{3-} in their coordination sphere. The combination of these two sites create a balanced emission spectrum under blue LED excitation, giving single phosphors that can result in pcLED lamps with lower CCTs (<4000 K) and good CRIs (>80). The efficiency of these phosphors at room temperature can be high, and the mechanisms for luminescence quenching at high temperatures will be discussed. The luminescence results reported here are significantly different than those in a prior literature report on $Si^{4+}-N^{3-}$ incorporation in $Y_3Al_5O_{12}:Ce^{3+}$ phosphors.[11] However, aspects of the results discussed here are similar to reports in the patent literature.[12−14]

2. Experimental Procedures

Powder phosphor samples were made using mixtures of high-purity Y_2O_3 (PIDC), Lu_2O_3 (PIDC), Tb_4O_7 (PIDC), CeO_2 (Alfa Aesar), α-Al_2O_3 (Ceralox), α-Si_3N_4 (Cerac), and AlF_3 (Alfa Aesar) and fired in N_2/H_2 mixtures at 1400−1550 °C for 5−10 h. The Si^{4+} in these compositions was provided by α-Si_3N_4, giving a slight excess of N^{3-}, and AlF_3 was added as a fluxing agent to improve the efficiency of these phosphors.[15] The compositions reported here are the nominal compositions based upon equivalent levels of Si^{4+} and N^{3-}. Powder X-ray diffraction (XRD) data were collected from $2\theta = 10-90°$ using Ni-filtered Cu Kα radiation on a Bruker D8 Advance diffractometer equipped with a linear position-sensitive detector (PSD-50m, M. Braun). Additionally, some measurements were carried out on a Bruker D8 Advance diffractometer equipped with a SOL-X energy-dispersive detector in the same angular range. NIST-certified SRM 640c silicon was used as an external calibration standard for lattice parameter measurements. Peak-to-background ratios for the strongest garnet reflection were greater than 500 for lattice parameter measurements with typical least-squares errors for the refined lattice parameters of 0.0001 Å or less. In practice, these least-squares errors are generally smaller than the "true" error calculated from refinements of the same sample scanned multiple times, ~0.0005 Å. The higher value is taken as the error for the lattice parameter measurements in this report.

Phosphor emission measurements were made on powders pressed into an aluminum plaque using a SPEX Fluorolog 3 with corrections for Xe lamp intensity and instrument response. Relative plaque quantum efficiency measurements used commercial garnet phosphors as standards and are corrected for sample absorption using $BaSO_4$ (Kodak) as a reflectance standard. Diffuse reflectance measurements for Ce^{3+}-doped samples used the same spectrometer with $BaSO_4$ as a reflectance standard. Diffuse reflectance measurements for undoped samples used a Perkin-Elmer Lambda 800 with $BaSO_4$ as a powder reflectance standard. High temperature luminescence intensity measurements used an Al plaque with cartridge heaters with the temperature measured by thermocouples inside the plaque and controlled by a standard Watlow temperature controller. Excitation spectra were recorded in a modified Cary 14 spectrophotometer, using the chopped radiation of either a tungsten-halogen (for visible/near-UV excitation) or a deuterium (for UV excitation) lamp as the excitation source with the emission detected by a Hamamatsu R212 photomultiplier tube (PMT) and appropriate narrow band interference filters. The signal was processed with a Stanford lock-in amplifier to increase the signal-to-noise ratio and suppress the PMT dark current. The excitation spectra were corrected for excitation photon flux using a calibrated Hamamatsu photodiode as a reference detector.

Time resolved measurements at room temperature used a tripled Nd:YAG laser at 355 nm (JDS Uniphase) coupled into an Edinburgh F900 spectrofluorometer with a Peltier cooled R928-P Hamamatsu photomultiplier tube (PMT) detector. The fwhm of the laser pulse convoluted with the overall system response is ~1 ns. Time resolved measurements from 77−800 K used a LED excitation source filtered through a narrow band interference filter (10 nm width) driven by the amplified (Avantec) pulses of an Avtech AVP-C pulse generator. The emission was filtered through a 0.5 m McPherson monochromator and detected with a Hamamatsu R212 PMT detector. The time-resolved fluorescence was recorded through a photon counting system, consisting of an Ortec 567 time-to-amplitude converter in conjunction with an EG&G pulse height analyzer. The temporal response for this experimental setup was measured at 2 ns.

The interaction between localized Ce^{3+} $5d^1$ levels and extended conduction band states has been analyzed by measuring the IR-stimulated luminescence (IRSL) after excitation at various wavelengths. This method is similar to thermoluminescence excitation spectroscopy,[16] but instead of heating the sample after excitation, an IR laser was used to depopulate trapped electrons. Phosphor samples are irradiated in a liquid N_2 cryostat at various temperatures using a 100 W Xe excitation source filtered by appropriate optical filters for wavelength selection. After excitation, the sample is excited by a Nd:YAG laser ($\lambda = 1064$ nm) to depopulate any filled traps; the IRSL was measured using a Hamamatsu model 1477−06 red sensitive PMT whose signal is recorded by a ComTech multichannel scaler card and is normalized to the incident UV/blue excitation intensity. In principle, the onset of the IRSL signal vs excitation wavelength gives the energy position of the Ce^{3+} $4f^1$ ground-state versus the conduction band.

3. Results and Discussion

Previous experiments estimated that Si^{4+} can replace ~12% of the tetrahedral Al^{3+} sites in YAG when N^{3-} is the charge compensating ion,[10] giving a garnet composition of $Y_3Al_{4.65}Si_{0.35}O_{11.65}N_{0.35}$. The results in this report on the solubility of $Si^{4+}-N^{3-}$ in YAG powders are similar. While garnets with compositions of $(Y_{0.97}Ce_{0.03})_3Al_{4.75}Si_{0.25}O_{11.75}N_{0.25}$ are single phase by X-ray diffraction (Figure 1a), nominal compositions of $(Y_{0.97}Ce_{0.03})_3Al_{4.5}Si_{0.5}O_{11.5}N_{0.5}$ are no longer single phase with secondary phases of $Y_2Si_3N_4O_3$ and $YAlO_3$. Using this synthesis method, the solubility of $Si^{4+}-N^{3-}$ into Al^{3+} garnets decreases with dodecahedral cation size and is limited in the Tb^{3+} garnets (Figure 1b), following the trends for phase stability in garnets, where larger dodecahedral cations and smaller tetrahedral cations generally destabilize garnet formation.[17] This report is not an exhaustive study on the solid solubility of $Si^{4+}-N^{3-}$ in garnet hosts, and different processing conditions (i.e., firing temperatures, atmospheres, starting materials, fluxes, etc.) could have some effect on the results reported here.

(11) Lin, Y. S.; Tseng, Y. H.; Liu, R. S.; Chan, J. C. C. *J. Electrochem. Soc.* **2007**, *154*, P16.
(12) Fiedler, T.; Fries, T.; Jermann, F.; Zachau, M.; Zwaschka, F. World Patent WO2005/061659A1, 2005.
(13) Schmidt, P. J.; Mayr, W.; Meyer J.; Schreinemacher, B. World Patent WO2006/095284A1, 2006.
(14) Setlur, A. A.; Bachniak, E. A. U. S. Patent Application 2006/0197443, 2006.
(15) Comanzo, H. A. U. S. Patent 6 409 938, 2002.
(16) Fleniken, J.; Wang, J.; Grimm, J.; Weber, M. J.; Happek, U. *J. Lumin.* **2001**, *94−95*, 465.
(17) Geller, S. *Z. Kristallogr.* **1967**, *125*, 1.

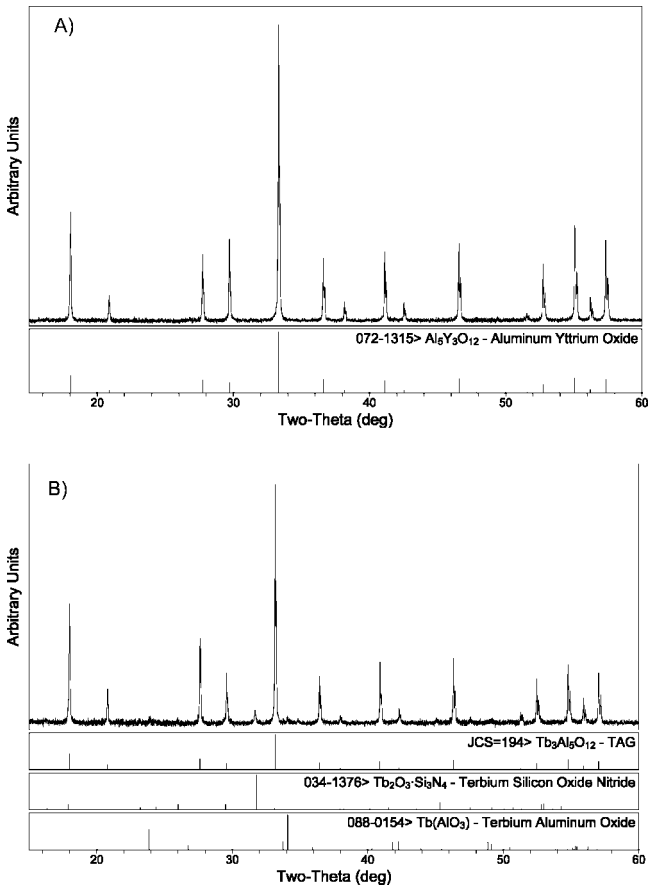

Figure 1. Powder X-ray diffraction patterns for (a) $(Y_{0.97}Ce_{0.03})_3Al_{4.9}Si_{0.1}O_{11.9}N_{0.1}$; and (b) $(Tb_{0.97}Ce_{0.03})_3Al_{4.9}Si_{0.1}O_{11.9}N_{0.1}$.

Table 1. Lattice Parameters of Garnet Compositions with and without $Si^{4+}-N^{3-}$

composition	lattice parameter (Å)
$Y_3Al_5O_{12}$	12.0066
$Y_3Al_{4.9}Si_{0.1}O_{11.9}N_{0.1}$	12.0045
$Y_3Al_{4.8}Si_{0.2}O_{11.8}N_{0.2}$	12.0030

The addition of $Si^{4+}-N^{3-}$ leads to a reduction in the garnet lattice parameter (Table 2), similar to previous results in the $BaAl_{2-x}Si_xO_{4-x}N_x$ system.[9] This reduction is likely due to the shorter bond lengths for tetrahedral $Si^{4+}-N^{3-}$ bonds (1.685−1.76 Å in Si_3N_4[18]) versus tetrahedral $Al^{3+}-O^{2-}$ bonds in YAG (1.761 Å[19]) as well as the smaller size of Si^{4+} versus Al^{3+}. The addition of $Si^{4+}-N^{3-}$ could also lead to longer dodecahedral and octahedral bond lengths because of the larger size of N^{3-} versus O^{2-}. Because the addition of Si^{4+}-N^{3-} to YAG affects the Ce^{3+} luminescence (vide infra), it would be helpful to quantify the bond lengths and extent of Si^{4+}/N^{3-} ordering in these powders. However, further characterization work, such as neutron diffraction, will be necessary since Si^{4+}/Al^{3+} and N^{3-}/O^{2-} have similar X-ray scattering factors making it difficult to distinguish between these ions in X-ray diffraction experiments.

Adding Si^{4+}-N^{3-} to $Lu_3Al_5O_{12}$:Ce^{3+} (LuAG), $Y_3Al_5O_{12}$:Ce^{3+} (YAG), and $Tb_3Al_5O_{12}$:Ce^{3+} (TbAG) phosphors changes the powder body color under fluorescent room light from yellow-green to yellow-orange. The change in the body occurs to a lesser extent in TbAG, due to significant second phase formation (Figure 1b). The orange body color is partially due to a distinct blue-green absorption band that is 2400−3000 cm^{-1} lower in energy versus the blue Ce^{3+} $4f^1 \rightarrow 5d^1$ absorption (Figure 2 and Table 1). The relative strength of this absorption band is correlated to the amount of $Si^{4+}-N^{3-}$ addition (Figure 2) and is therefore assigned to the lowest energy $4f^1 \rightarrow 5d^1$ transition of Ce^{3+} ions that have N^{3-} in their nearest neighbor coordination. While the addition of Si^{4+} in aluminate garnets redshifts the energy of the lowest Ce^{3+} $5d^1$ level,[7,20] the presence of N^{3-} is critical in these samples. Samples with similar levels of Si^{4+} replacing Al^{3+} on tetrahedral sites but with Ca^{2+} in dodecahedral sites or Mg^{2+} in octahedral sites for charge compensation do not have similar low energy absorption bands. In addition, these additional Ce^{3+} absorption bands were not observed when we attempted to incorporate N^{3-} via AlN but without Si^{4+} charge compensation. It is therefore likely that some degree of $Si^{4+}-N^{3-}$ ordering is present in these samples.

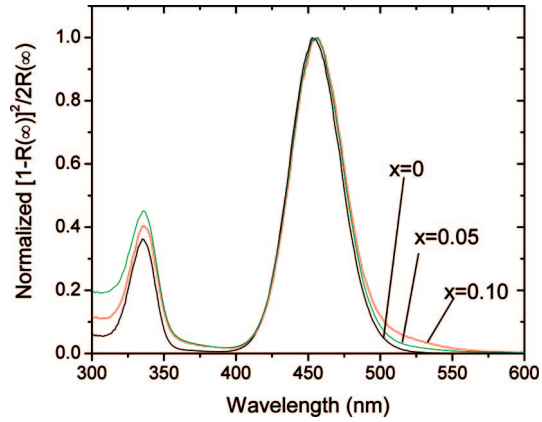

Figure 2. Normalized reflectance spectra of $(Y_{0.97}Ce_{0.03})_3Al_{5-x}Si_xO_{12-x}N_x$ after the Kubelka−Munk transformation, $[1 - R(\infty)]^2/2R(\infty)$, of the reflectance data.

Table 2. Position of the Lowest Energy $4f^1 \rightarrow 5d^1$ Ce^{3+} Absorption in Typical Al^{3+} Garnets and Those Doped with $Si^{4+}-N^{3-}$

host	typical Ce^{3+} in garnets (cm^{-1})	Ce^{3+}coordinated by Si^{4+}-N^{3-} (cm−1)	energy difference (cm−1)
LuAG	22 480	20 040	2440
YAG	21 940	19 170	2770
TbAG	21 740	18 630	3100

The redshift in the position of the lowest $4f^1 \rightarrow 5d^1$ Ce^{3+} absorption when N^{3-} is coordinated to Ce^{3+} is likely due to a shift in the Ce $5d^1$ centroid from both the higher covalency and polarizability of Ce^{3+}-N^{3-} bonds versus $Ce^{3+}-O^{2-}$ bonds[8]. The low-energy tail in the UV Ce^{3+} $4f^1 \rightarrow 5d^1$ absorption band for samples with $Si^{4+}-N^{3-}$ (Figure 2) is potential evidence for a shift in the Ce^{3+} $5d^1$ centroid. However, there are no higher energy $4f^1 \rightarrow 5d^1$ excitation bands that can be assigned exclusively to Ce^{3+} ions with N^{3-} in their nearest neighbor coordination (vide infra). Therefore, the assignment for the redshift in the lowest Ce^{3+}

(18) Billy, M.; Labbe, J. C.; Selvaraj, A.; Roult, G. *Mater. Res. Bull.* **1983**, *18*, 921.
(19) Euler, F.; Bruce, J. A. *Acta Crystallogr.* **1965**, *19*, 971.
(20) Robertson, J. M.; van Tol, M. W.; Smits, W. H.; Heynen, J. P. H. *Philips J. Res.* **1981**, *36*, 15.

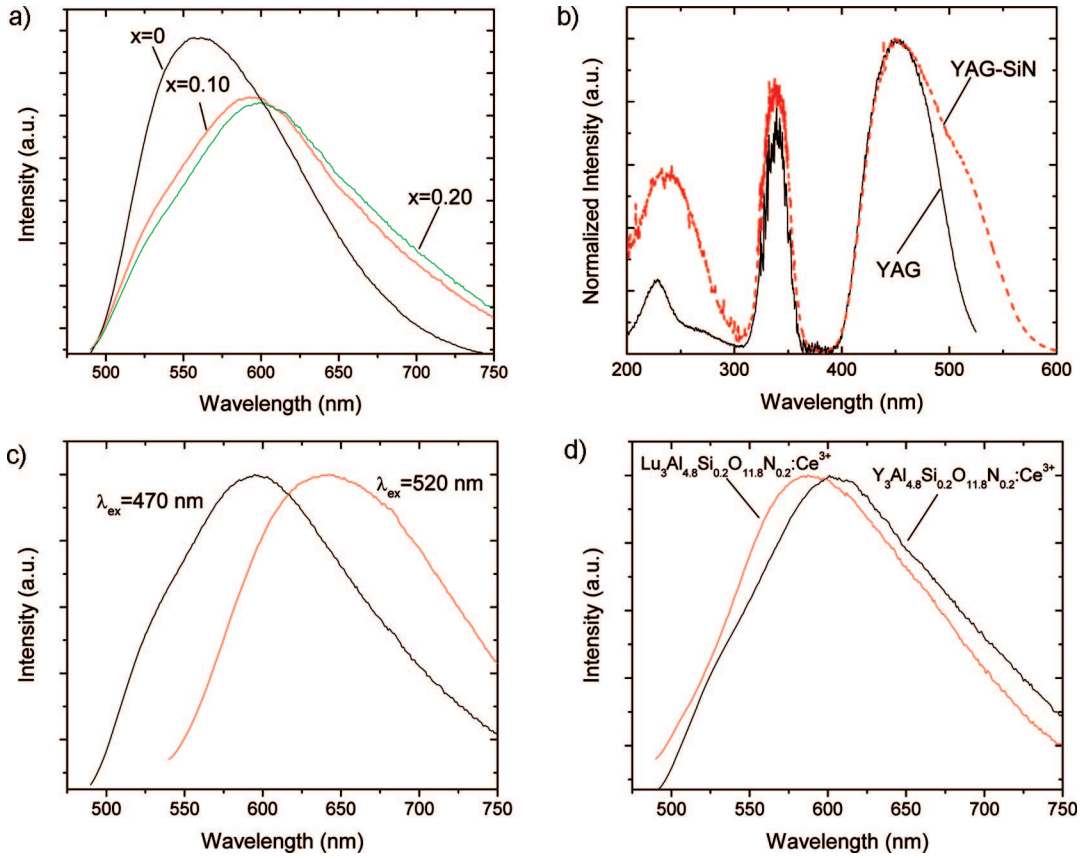

Figure 3. (a) Room-temperature emission spectra ($\lambda_{ex} = 470$ nm) of $(Y_{0.97}Ce_{0.03})_3Al_{5-x}Si_xO_{12-x}N_x$; (b) Room temperature excitation spectrum for Ce^{3+} ions with N^{3-} in its coordination sphere in $(Y_{0.97}Ce_{0.03})_3Al_{4.9}Si_{0.1}O_{11.9}N_{0.1}$ ($\lambda_{em} = 720$ nm; denoted as YAG-SiN) compared to the excitation spectrum for $(Y_{0.97}Ce_{0.03})_3Al_5O_{12}$ ($\lambda_{em} = 560$ nm; denoted as YAG); (c) Room temperature emission spectra versus excitation wavelength for $(Y_{0.97}Ce_{0.03})_3Al_{4.9}Si_{0.1}O_{11.9}N_{0.1}$; and (d) Room temperature emission spectra ($\lambda_{ex} = 470$ nm) of $(Lu_{0.97}Ce_{0.03})_3Al_{4.8}Si_{0.2}O_{11.8}N_{0.2}$ and $(Y_{0.97}Ce_{0.03})_3Al_{4.8}Si_{0.2}O_{11.8}N_{0.2}$.

$4f^1 \rightarrow 5d^1$ absorption band when N^{3-} is in its coordination sphere to only covalency and polarizability is speculative at this time. Also, given the relatively low levels of N^{3-} substitution, we assume that the Ce^{3+} ions with lower energy $4f^1 \rightarrow 5d^1$ absorption bands have only one nearest neighbor O^{2-} ions replaces by N^{3-}. The presence of just one additional absorption band with the addition of $Si^{4+}-N^{3-}$ (Figure 2) supports this assumption.

The additional low energy absorption band due to Si^{4+}-N^{3-} in these aluminate garnets is also reflected in a broader $5d^1 \rightarrow 4f^1$ Ce^{3+} emission band that has a strong red spectral component (Figure 3a). The relative intensity of this red spectral component is correlated with the $Si^{4+}-N^{3-}$ doping level and allows for single phosphor pcLEDs with CCTs less than 4000 K and CRIs greater than 80.[12−14] The excitation spectra of these phosphors again indicate the presence of at least two distinct sites with higher and lower energy $4f^1 \rightarrow 5d^1$ Ce^{3+} excitation bands in the blue and blue-green (Figure 3b). The position of the additional excitation band for red emission is in agreement with the position of the low energy absorption band (Figure 2). Therefore, the additional red emission in these phosphors is assigned to Ce^{3+} ions with N^{3-} in its nearest neighbor coordination. The emission spectrum under green excitation ($\lambda_{ex} = 520$ nm) for $(Y_{0.97}Ce_{0.03})_3Al_{4.9}Si_{0.1}O_{11.9}N_{0.1}$ has a maximum at 620−630 nm (Figure 3c), giving a Stokes shift for Ce^{3+} ions with N^{3-} in their coordination sphere of ~3500 cm^{-1}, larger than our previous measurements for the Stokes shift (~2400 cm^{-1}) for typical aluminate garnets.[21] Apart from varying the $Si^{4+}-N^{3-}$ level, it is also possible to modify the emission color of these phosphors through dodecahedral site modifications; the emission of YAG-based phosphors is red-shifted versus LuAG-based phosphors (Figure 3c), in agreement with both the position of the lowest-energy $5d^1$ levels in absorption (Table 2) and the compositional trends for Al^{3+} garnets without $Si^{4+}-N^{3-}$.[20]

Analysis of the excitation and emission spectra give evidence for energy transfer between typical (i.e., high energy and not coordinated with N^{3-}) and low energy (coordinated with N^{3-}) Ce^{3+} ions in these garnets. First, even at low $Si^{4+}-N^{3-}$ levels, the Ce^{3+} emission spectrum under the excitation of typical Ce^{3+} ions is strongly weighted toward emission of the low energy Ce^{3+} ions (Figure 3a). In addition, the excitation spectrum for the low energy emission band has a component that is similar to the excitation/absorption band of high energy Ce^{3+} ions in garnets (Figure 3a). Dipole−dipole energy transfer between the high and low energy Ce^{3+} ions in these materials is expected because of the large spectral overlap (~0.5 eV^{-1}) between the $5d^1 \rightarrow 4f^1$ emission of the higher-energy Ce^{3+} ions and the low energy $4f^1 \rightarrow 5d^1$ absorption of Ce^{3+} ions with N^{3-} in its

(21) Setlur, A. A.; Srivastava, A. M. *Opt. Mater.* **2007**, *29*, 1647.

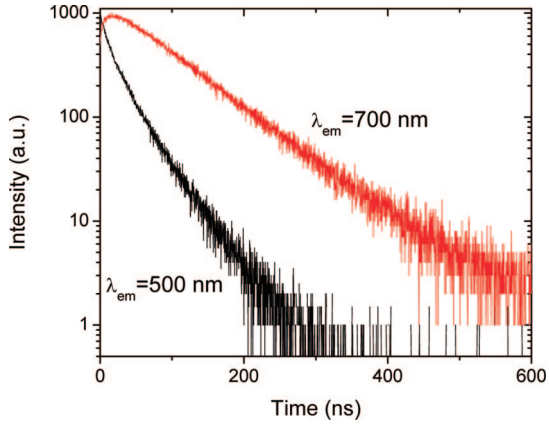

Figure 4. Room-temperature decay profiles (λ_{ex} = 355 nm) for $(Lu_{0.97}Ce_{0.03})_3Al_{4.8}Si_{0.2}O_{11.8}N_{0.2}$ taken at various emission wavelengths.

coordination sphere (Figures 2 and 3a). This spectral overlap gives a critical distance, R_c, of 20.5 Å and a critical concentration, x_c, of ~0.015 using[22,23]

$$R_c^6 = (6.3\times10^{27})(4.8\times10^{-16})E^{-4}fSO \quad (1)$$

$$x_c = \frac{6V}{\pi N R_c^3} \quad (2)$$

where f is the oscillator strength of the Ce^{3+} absorption transition (~0.0015[24]), SO is the spectral overlap of the high energy ($5d \rightarrow {}^2F_{5/2}$) Ce^{3+} emission and the low-energy Ce^{3+} excitation, E is the energy of maximum overlap (2.35 eV), V is the unit cell volume (1687 Å^3 [19]), and N is the number of dodecahedral sites in a garnet unit cell (24[19]). The calculated critical concentration is below the concentration of Ce^{3+} ions with a N^{3-} nearest neighbor assuming a random distribution of Ce^{3+} and N^{3-} ions. However, energy migration between Ce^{3+} ions[21] will further increase the probability for energy transfer between high and low energy Ce^{3+} ions.

Direct experimental evidence for energy transfer is given by time-resolved measurements (Figure 4). At high emission energies (λ_{em} = 500 nm), the decay profile of $(Lu_{0.97}Ce_{0.03})_3Al_{4.8}Si_{0.2}O_{11.8}N_{0.2}$ is multiexponential with initial fast components ($t_{1/2} \approx$ 12 ns), and the decay time at long times is similar to the 57 ns decay time of isolated Ce^{3+} ions in LuAG:Ce^{3+} [21]. At lower emission energies (λ_{em}= 700 nm), the decay time is ~85 ns with a build-up characterized by a time constant is ~15 ns. The similar time constants for the fastest decay component of the high energy emission and the build-up of the low energy emission demonstrates that energy transfer occurs between high energy Ce^{3+} ions in garnets and lower energy Ce^{3+} ions with N^{3-} in their coordination sphere. The longer radiative lifetime for Ce^{3+} ions coordinated by N^{3-} is also in general agreement with the relationship between emission wavelength and the radiative rate for the electric dipole allowed Ce^{3+} $5d^1 \rightarrow 4f^1$ transition in garnets.[21]

While these phosphors have desirable spectral properties, the phosphor efficiency must be high for practical use and potential limitations should be understood for lamp optimization. Initial samples of these phosphors have a room temperature quantum efficiency that is greater than 80% of commercial Ce^{3+} garnet phosphors. However, under green excitation (λ_{ex} = 520 nm) that primarily excites low-energy Ce^{3+} ions, there is a reduction in emission intensity at higher temperature with a larger reduction in YAG-based versus LuAG-based phosphors (Figure 5a). The decay time under green excitation in $(Y_{0.97}Ce_{0.03})_3Al_{4.9}Si_{0.1}O_{11.9}N_{0.1}$ also shows slight quenching (<10%) between 77 and 300 K with strong quenching for T > 300 K, in reasonable agreement with the emission measurements (Figure 5b). In comparison, typical Ce^{3+} ions in LuAG and YAG can have little to no emission quenching beyond ~150 °C [25−27] (Figure 5b). The weak quenching at low temperatures could be due to energy transfer to a lattice defect or an impurity. This is important at high temperatures in typical Ce^{3+} doped aluminate garnets without $Si^{4+}-N^{3-}$[27] and could be reduced or eliminated by improved synthesis procedures as with other nitride phosphors.[28] However, the relatively low concentration of Ce^{3+} ions coordinated with N^{3-} leads us to assume that significant quenching due to energy migration between Ce^{3+} ions coordinated with N^{3-} is limited. We therefore believe that the luminescence quenching above room temperature for Ce^{3+} ions with N^{3-} in its coordination sphere is more intrinsic in nature. The implications for the thermal quenching of Ce^{3+} ions coordinated with N^{3-} under typical blue excitation (primarily into the $4f^1 \rightarrow 5d^1$ absorption band of high energy Ce^{3+} ions) are significant intensity losses and a blueshift in the phosphor emission spectrum at higher temperatures (Figure 5c). The high-temperature emission spectra for these garnets with $Si^{4+}-N^{3-}$ under blue excitation resemble those of the pure aluminate garnets without the addition of $Si^{4+}-N^{3-}$. The relatively strong luminescence quenching could therefore limit practical use of these phosphors in many pcLED packages.

The possible causes for thermally activated nonradiative transitions in Ce^{3+} are photoionization into the host lattice conduction band or level crossing between the lowest energy $5d^1$ level and the $4f^1$ ground states. Enhanced quenching via photoionization for Ce^{3+} ions coordinated with N^{3-} requires a relatively small energy barrier between the lowest $5d^1$ level and conduction band states. $Y_3Al_{4.9}Si_{0.1}O_{11.9}N_{0.1}$ powders have a strong absorption band whose onset is at ~295 nm (~4.2 eV), whereas $Y_3Al_5O_{12}$ powders made under similar conditions do not have any strong absorption bands for wavelengths greater than 200 nm (~6.2 eV) (Figure 6a), in agreement with the experimental bandgap for YAG as measured by X-ray photoelectron spectroscopy, ~6.5−7 eV.[29] A similar low energy absorption band has also been measured in $BaAl_{2-x}Si_xO_{4-x}N_x$,[9] indicating an intrinsic absorption band related to the incorporation of $Si^{4+}-N^{3-}$

(22) van Schaik, W.; Lizzo, S.; Smit, W.; Blasse, G. *J. Electrochem. Soc.* **1993**, *140*, 216.
(23) Blasse, G. *Philips Res. Rep.* **1969**, *24*, 131.
(24) Tomiki, T.; Kohatsu, T.; Shimabukuro, H.; Ganaha, Y. *J. Phys. Soc. Jpn.* **1992**, *61*, 2382.
(25) Robbins, D. J. *J. Electrochem. Soc.* **1979**, *126*, 1550.
(26) Lyu, L.-J.; Hamilton, D. S. *J. Lumin.* **1991**, *48−49*, 251.
(27) Bachmann, V. M. Studies on Luminescence and Quenching Mechanisms in Phosphors for Light Emitting Diodes. Ph.D. Thesis, Utrecht Universiteit, Utrecht, The Netherlands, 2007.
(28) Xie, R.-J.; Hirosaki, N.; Suehiro, T.; Xu, F.-F.; Mitomo, M. *Chem. Mater.* **2006**, *18*, 5578.
(29) Thiel, C. W.; Cruguel, H.; Wu, H.; Sun, Y.; Lapeyre, G. J.; Cone, R. L.; Equall, R. W.; Macfarlane, R. M. *Phys. Rev. B* **2001**, *64*, 085107.

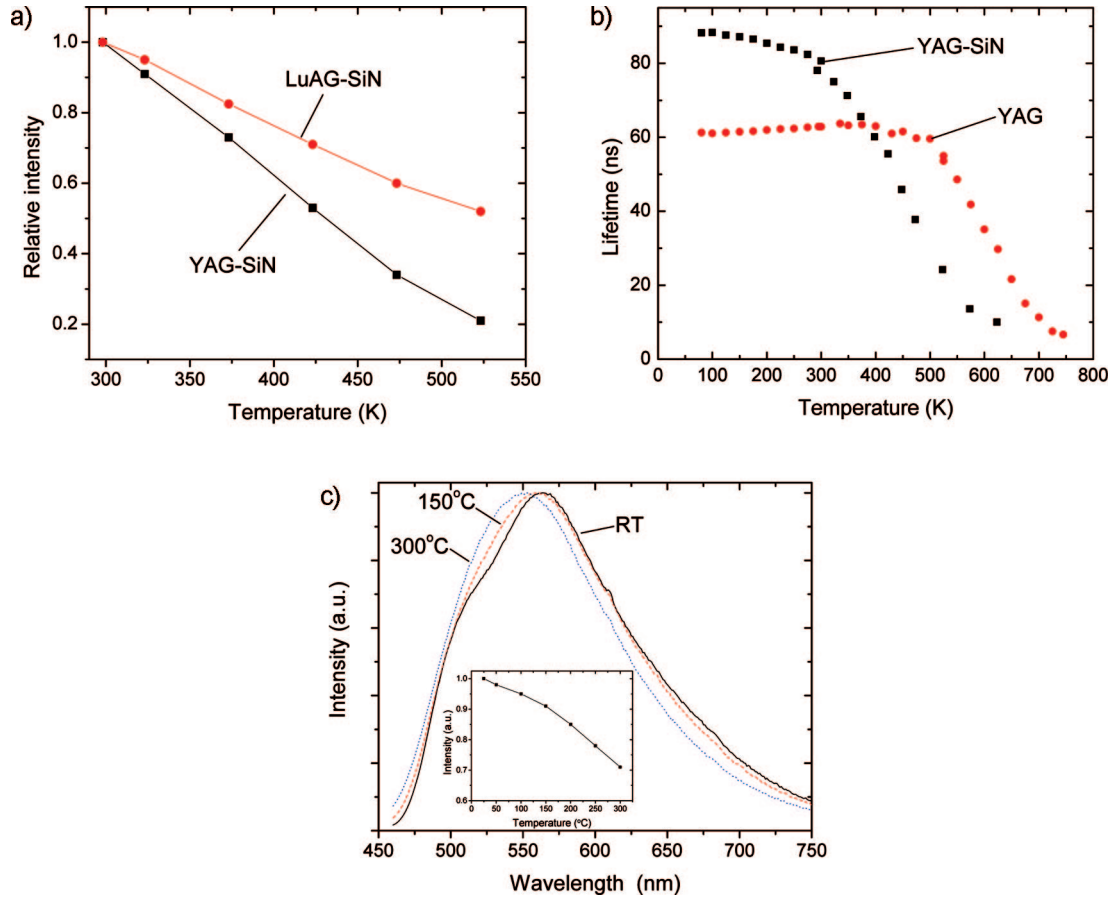

Figure 5. (a) Relative emission intensity versus temperature under green excitation (λ_{ex} = 520 nm) for $(Y_{0.97}Ce_{0.03})_3Al_{4.9}Si_{0.1}O_{11.9}N_{0.1}$ (denoted as YAG-SiN) and $(Lu_{0.97}Ce_{0.03})_3Al_{4.8}Si_{0.2}O_{11.8}N_{0.2}$ (denoted as LuAG-SiN). The spectral range used for the integrated intensity is from 700 to 750 nm to reduce the overlap with typical, high-energy Ce^{3+} ions. (b) Decay time versus temperature for $(Y_{0.97}Ce_{0.03})_3Al_5O_{12}$ (λ_{ex} = 470 nm; λ_{em} = 560 nm; denoted as YAG) and the lower energy site in $(Y_{0.97}Ce_{0.03})_3Al_{4.9}Si_{0.1}O_{11.9}N_{0.1}$ (λ_{ex} = 520 nm, λ_{em} = 750 nm; denoted as YAG-SiN). (c) Normalized emission spectra (λ_{ex}= 470 nm) versus temperature for $(Lu_{0.99}Ce_{0.01})_3Al_{4.8}Si_{0.2}O_{11.8}N_{0.2}$. The inset shows the integrated intensity versus temperature for these measurements.

in aluminate hosts. This absorption band is also observed in the Ce^{3+} excitation spectrum for YAG with $Si^{4+}-N^{3-}$ (Figure 3b), further supporting the intrinsic nature of this absorption band. Since the absorption edge for various Y−Si−O−N compounds range from ~245−285 nm (4.35−5.1 eV),[30] we initially assign this absorption band in $Y_3Al_{4.8}Si_{0.2}O_{11.8}N_{0.2}$ to a bandgap transition associated with the incorporation of $Si^{4+}-N^{3-}$. The $Si^{4+}-N^{3-}$ incorporation might lower the photoionization threshold of Ce^{3+}, but our IR stimulated luminescence (IRSL) measurements at room temperature and 80 K show no IRSL for excitation energies less than 20 000 cm^{-1} (500 nm) with stronger IRSL for excitation energies greater than 28 570 cm^{-1} (350 nm) (Figure 6b). The IRSL signal increases with temperature for UV excitation; this likely indicates some thermal barriers for photoionization after excitation into higher energy Ce^{3+} $5d^1$ levels. However, there is little to no IRSL when exciting into the lowest $5d^1$ level of either low energy or high energy Ce^{3+} ions. Therefore, we propose that Ce^{3+} photoionization is not occurring after excitation into the lowest $5d^1$ level of Ce^{3+} and that level crossing is the key factor for the stronger quenching of Ce^{3+} ions coordinated with N^{3-}. Further experimental work is necessary to exactly place the energy position of the $4f^1$ ground state for Ce^{3+} ions coordinated with N^{3-} with respect to the local bandgap to understand the different energy barriers for Ce^{3+} photoionization in these phosphors.

Assigning the quenching of Ce^{3+} ions coordinated with N^{3-} to nonradiative level crossing between the excited $5d^1$ level and the low energy $4f^1$ levels explains the relative compositional trends for luminescence quenching similar to the analysis for $(Y,Gd)_3Al_5O_{12}:Ce^{3+}$ garnet phosphors.[27,31] The lower $5d^1$ energy for Ce^{3+} ions coordinated with N^{3-} combined with a larger Stokes shift reduces the energy barrier for nonradiative crossovers from the $5d^1$ level to the $4f^1$ ground states, resulting in the stronger quenching of Ce^{3+} ions coordinated by N^{3-}. Also, the stronger quenching in YAG-based versus LuAG-based phosphors with $Si^{4+}-N^{3-}$ (Figure 5a) is because the lower-energy position for the excited $5d^1$ state in YAG-based phosphors (Table 2) reduces the energy barrier for level crossing.

4. Conclusions

In this report, the luminescence of Ce^{3+} doped garnets when N^{3-} replaces O^{2-} with charge compensation by Si^{4+}

(30) van Krevel, J.W. H. On New Rare Earth Doped M-Si-Al-O-N Materials: Luminescence Properties and Oxidation Resistance. Ph.D. Thesis, Technische Universiteit Eindhoven, Eindhoven, The Netherlands, 2000.

(31) Chiang, C.-C.; Tsai, M.-S.; Hon, M.-H. *J. Electrochem. Soc.* **2008**, *155*, B517.

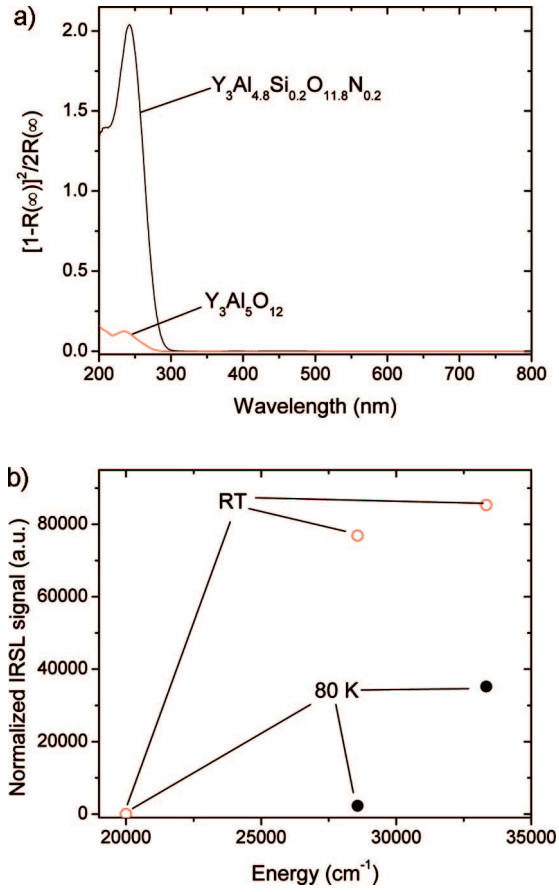

Figure 6. (a) Diffuse reflectance after Kubelka−Munk transformation of $Y_3Al_{4.9}Si_{0.2}O_{11.8}N_{0.2}$ versus $Y_3Al_5O_{12}$ (with nominal Tb^{3+}/Ce^{3+} impurities). (b) Infrared stimulated luminescence (IRSL) intensity versus excitation wavelength for $(Y_{0.97}Ce_{0.03})_3Al_{4.9}Si_{0.1}O_{11.9}N_{0.1}$ at 80 K (closed circles) and room temperature (open circles). The absence of an IRSL signal for low energy excitation is an indication that photoionization does not occur after excitation into the lowest $5d^1$ level of the low and high energy Ce^{3+} ions.

replacement of Al^{3+} on the tetrahedral sites are discussed and analyzed. The incorporation of N^{3-} anions leads to Ce^{3+} ions whose lowest 5d excited state is at lower energy compared to typical garnets, as expected given the lower electronegativity of N^{3-} versus O^{2-}. Evidence is presented for energy transfer between typical Ce^{3+} ions in the garnet and those coordinated by N^{3-}, giving a strong red component in the emission spectra under blue excitation. When combined with blue LEDs, these phosphors can give single phosphor pcLEDs with CCT*s* < 4000 K and CRIs > 80. There is the potential limitation that the low energy Ce^{3+} ions coordinated by N^{3-} have stronger luminescent quenching versus typical Ce^{3+} ions in garnets. In practical terms, this could affect both the lamp efficacy and color depending on the LED lamp design and operating conditions.

Acknowledgment. The authors thank E. A. Bachniak, M. C. Hill, S. J. Camardello, and C. S. Henderson for sample synthesis and initial luminescence measurements; J. J. Shiang for experimental assistance with the room-temperature decay measurements; and E. Radkov for a critical reading of the manuscript. This work was primarily supported by GE Lumination LLC with partial support of the spectroscopic measurements by the U.S. Department of Energy through Contracts DE-FC26-04NT41945 and DE-FC26-06NT42934. This report was prepared as an account of work sponsored by an agency of the United States Government. Neither the United States Government nor any agency thereof, nor any of their employees, makes any warranty, express or implied, or assumes any legal liability or responsibility for the accuracy, completeness, or usefulness of any information, apparatus, product, or process disclosed, or represents that its use would not infringe privately owned rights. Reference herein to any specific commercial product, process, or service by trade name, trademark, manufacturer, or otherwise does not necessarily constitute or imply its endorsement, recommendation, or favoring by the United States Government or any agency thereof. The views and opinions of authors expressed herein do not necessarily state or reflect those of the United States Government or any agency thereof.

CM801732D